



1 **Seasonal and interannual Dissolved Organic Carbon transport process dynamics in a**
2 **subarctic headwater catchment revealed by high-resolution measurements.**

3 Danny Croghan¹, Pertti Ala-Aho², Jeffrey Welker^{1,3,4}, Kaisa-Riikka Mustonen¹, Kieran
4 Khamis⁵, David M. Hannah⁵, Jussi Vuorenmaa⁶, Bjørn Kløve², and Hannu Marttila²

- 5 (1) Ecology and Genetics Research Unit, University of Oulu, Oulu, Finland
6 (2) Water, Energy and Environmental Engineering Research Unit, University of Oulu, Oulu,
7 Finland
8 (3) Department of Biological Sciences, University of Alaska Anchorage, USA
9 (4) UArctic, Rovaniemi, Finland
10 (5) School of Geography, Earth and Environmental Sciences, University of Birmingham,
11 Birmingham, UK
12 (6) Finnish Environment Institute, Finland
13

14 Corresponding Author: Danny Croghan (danny.croghan@oulu.fi)
15
16
17
18
19
20
21
22
23
24
25
26
27
28
29
30
31
32
33



34 **Abstract**

35 Dissolved organic carbon (DOC) dynamics are evolving in the rapidly changing Arctic and a
36 comprehensive understanding of the controlling processes is urgently required. For
37 example, the transport processes governing DOC dynamics are prone to climate driven
38 alteration given their strong seasonal nature. Hence, high-resolution and long-term studies
39 are required to assess potential seasonal and inter-annual changes in DOC transport
40 processes. In this study, we monitored DOC at a 30-minute resolution from September 2018
41 to December 2022 in a headwater peatland-influenced stream in Northern Finland (Pallas
42 catchment, 68° N). To assess transport processes multiple methods were used:
43 concentration – discharge (C-Q) slope for seasonal analysis, a modified hysteresis index for
44 event analysis, yield analysis, and random forest regression models to determine the
45 hydroclimatic controls on transport. The findings reveal the following distinct patterns: (a)
46 the slope of the C-Q relationship displays a strong seasonal trend, indicating increasing
47 transport limitation each month after snowmelt begins; (b) the hysteresis index decreases
48 post-snowmelt, signifying the influence of distal sources and DOC mobilization through
49 slower pathways; and (c) interannual variations in these metrics are generally low, often
50 smaller than month-to-month fluctuations. These results highlight the importance of long-
51 term and detailed monitoring to enable separation of inter and intra annual variability to
52 better understand the complexities of DOC transport. This study contributes to a broader
53 comprehension of DOC transport dynamics in the Arctic because knowledge gained
54 regarding the dominant transport mechanisms and their seasonal variations is vital for
55 evaluating how the carbon cycle will change in the future in Arctic ecosystems.

56

57

58

59

60

61

62

63



64 **1. Introduction**

65 The dynamics of Dissolved Organic Carbon (DOC) in Arctic catchments are undergoing
66 profound transformations due to the impacts of climate change, recovery from acidification,
67 and land-use change (Anderson et al., 2023; de Wit et al., 2016; Liu et al., 2022; McGuire et al.,
68 2018; Shogren et al., 2021; Tank et al., 2016). Notably, the Arctic region has experienced a
69 fourfold increase in warming compared to the global average since 1979 (Rantanen et al.,
70 2022), fostering substantial changes in hydrological processes, particularly in terms of
71 transport mechanisms (Liu et al., 2022). Climate change-induced alterations are occurring in
72 permafrost extent (Koch et al., 2022), snowpack water storage (Bokhorst et al., 2016;
73 Pulliainen et al., 2020), snowpack duration (Bowering et al., 2023), snowmelt timing (Tan et
74 al., 2011), and hydrological seasonality (Osuch et al., 2022), which have been significantly
75 affecting DOC dynamics (Liu et al., 2022; Shogren et al., 2021). Consequently, these shifts
76 have triggered rapid and consequential transformations within both the Arctic water and
77 carbon cycles that are both climatically sensitive (Bintanja and Andry, 2017; Bruhwiler et al.,
78 2021; McGuire et al., 2009; Vihma et al., 2016).

79 DOC transport processes in the Arctic exhibit pronounced seasonality and are highly
80 susceptible to change (Bowering et al., 2023; Csank et al., 2019; Shatilla and Carey, 2019).
81 Among the various transport mechanisms, the spring snowmelt flood is the main event and
82 control on annual DOC flux in Arctic catchments (Croghan et al., 2023). Several studies have
83 demonstrated its contribution ranging from 37% to 82% of the annual DOC load, albeit with
84 considerable variations between catchments and years (Dyson et al., 2011; Finlay et al.,
85 2006; Prokushkin et al., 2011). However, in the Arctic, climate change is reducing snow
86 cover duration and increasing the fraction of precipitation in the liquid phase (Bintanja and
87 Andry, 2017). Consequently, storm events are emerging as increasingly important
88 mechanisms for the export of DOC from terrestrial catchments to streams (Day and Hodges,
89 2018; Speetjens et al., 2022). Furthermore, the lengthening growing seasons, accompanied
90 by potential increases in DOC source supply, are further exacerbating the impact of summer
91 and autumn storm events on DOC dynamics in the Arctic region (Bowering et al., 2020;
92 Pearson et al., 2013). Additionally, while the significance of shoulder seasons (defined in the
93 Arctic as the transitional period between the end of plant senescence and the freezing of
94 the headwaters, and after the onset of thaw till the end of snowmelt) for DOC export has



95 been acknowledged in recent years, their characterization remains limited. Therefore, there
96 is a pressing need for more extensive documentation to elucidate the influence of shifting
97 climate on DOC dynamics in the Arctic (Shogren et al., 2020).

98 Headwater catchments play a crucial role in the transport of DOC into streams (Fork et al.,
99 2020; Lambert et al., 2014). These catchments constitute approximately 90% of the total
100 global stream length and serve as the primary connection for carbon transport between
101 terrestrial landscapes and oceans (Argerich et al., 2016; Li et al., 2021). Allochthonous inputs
102 into the stream, driven by rain and snowmelt events, dominate the dynamics of headwater
103 catchments (Billett et al., 2006; Laudon et al., 2004). Headwater wetland mires are
104 especially abundant in northern latitudes and are significant contributors of carbon to the
105 stream, often exhibiting higher concentrations compared to other landscape types
106 (Campeau and del Giorgio, 2014; Dick et al., 2015; Gómez-Gener et al., 2021). Furthermore,
107 the seasonal dynamics of carbon transfer processes in headwater wetlands differ
108 significantly depending on the season. During snowmelt, rapid superficial pathways are
109 observed, which later evolve into more complex pathways in the landscape during the
110 summer and autumn (Croghan et al., 2023; Laudon et al., 2011). Additionally, headwater
111 catchments are highly vulnerable to the impacts of hydrological extremes (Koch et al.,
112 2022), and they are expected to undergo significant changes due to climate change (Ward et
113 al., 2020). The increasing hydrological stochasticity in Arctic catchments (e.g. occurrence
114 and magnitude of extremes) highlight the need to better understand inter-annual variability
115 using more highly resolved data to characterize event dynamics (Bring et al., 2016).
116 Consequently, longer term and higher frequency study of sensitive headwater catchments is
117 essential to better understand their functioning and response to environmental changes,
118 especially in high latitude conditions (Bruhwiler et al., 2021; Marttila et al., 2022, 2021).

119 To comprehensively investigate the transport processes of DOC across seasons, it is
120 essential to employ high-resolution, long-term monitoring approaches (Shogren et al.,
121 2020). This need is particularly pronounced in headwater environments, where the majority
122 of the DOC input into streams occurs during storm events and snowmelt (Billett et al.,
123 2006). Only through high-frequency monitoring can we adequately identify and understand
124 the transport processes and characteristics associated with sudden episodic and
125 unpredictable storm and snowmelt events, capturing the necessary resolutions for



126 improved process understanding (Blaen et al., 2016). Furthermore, higher-resolution data
127 collection can facilitate the use of multiple analytical techniques, such as hysteresis analysis,
128 which can offer deeper insights into DOC transport dynamics (Croghan et al., 2023; Lloyd et
129 al., 2016b). Historically, limited spatial and temporal field sampling has led to biases in our
130 understanding of the impacts of climate change in Arctic regions (Metcalf et al., 2018;
131 Shogren et al., 2020). Additionally, high-frequency DOC measurements in the Arctic remain
132 relatively rare, especially datasets that cover the shoulder seasons and encompass multi-
133 year measurements for assessing inter-annual differences (Beel et al., 2021; Shogren et al.,
134 2021). Hence, there is an urgent need to integrate high-frequency monitoring sites in
135 subarctic, low Arctic, and high Arctic regions, particularly for evaluating the ongoing
136 evolution of the Arctic carbon and water cycles (Laudon et al., 2017; Marttila et al., 2021;
137 Pedron et al., 2023).

138 To address key knowledge gaps in Arctic headwater DOC transport, our study focused on a
139 peatland-influenced headwater catchment located in subarctic, Northern Finland (68°N),
140 with the overarching aim to identify the primary drivers of transport processes of DOC and
141 explore their seasonal and interannual dynamics. We utilized a unique four-year high-
142 resolution dataset of DOC, allowing us to conduct high-frequency analyses. To enhance
143 understanding of DOC transport processes in the Arctic and their implications for future
144 dynamics the following interlinked research questions were addressed:

- 145 1) How do the main drivers of DOC transport processes vary across different seasons?
- 146 2) To what extent do DOC transport processes and their drivers vary inter-annually?

147

148 **2.0 Methods**

149

150 **2.1 Site Description**

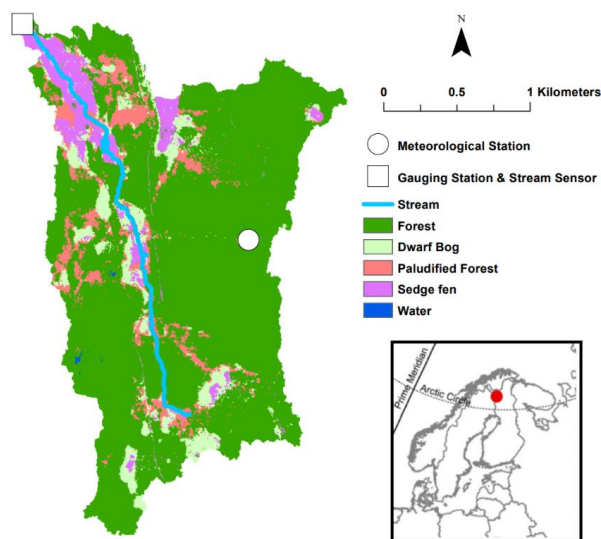
151 The research was conducted within the Lompolojängänoja catchment, also referred to as
152 the Pallas catchment (Marttila et al., 2021), situated in a peatland-influenced headwater
153 stream (Figure 1). This catchment is located in Northern Finland (68°02'N, 24°16'W) within
154 the Pallas-Yllästunturi National Park. Encompassing a total area of 4.42 km², the Pallas
155 catchment exhibits elevations ranging from 268 m to 375 m above sea level.

156 The stream location is strongly influenced by a peatland, which comprises fens, mires,
157 paludified forest and floodplains. This peatland exerts significant control over the flow



158 dynamics within the catchment, contributing most of the flow at the headwater location
159 (Marttila et al., 2021). Within the broader catchment area, coniferous forests account for
160 79% of the land classification, followed by mixed forests (9%) and peatbogs (8%).

161 The Pallas catchment is categorized as subarctic, characterized by long winters with
162 substantial snowfall and short, rainy summers. Notably, despite its northern latitude, the
163 catchment lacks a permafrost layer, making it one of the most northern research
164 catchments without permafrost (Marttila et al., 2021). The mean annual rainfall in the
165 catchment amounts to 521 mm, with 42% of that precipitation occurring as snowfall.
166 Typically, snowmelt occurs towards the end of April or early May and concludes by late May
167 or early June. Permanent snow cover in the catchment typically commences around late
168 October, though it can extend into late November. For further comprehensive descriptions
169 of the Pallas catchment's characteristics, please refer to Marttila et al., (2021).



170

171 **Figure 1** – Map of the study location (inset), catchment and measurement locations within
172 the catchment. Classification of vegetation in the catchment was derived from (Räsänen et
173 al., 2021)

174 **2.2 Stream Monitoring**

175 The monitoring of stream variables was conducted during the period from 18th September
176 2018 to 31st December 2022. To measure these variables, a multiparameter sonde (YSI-



177 EXO3; Excitation 365 nm, Emission 480 nm) was deployed at the catchment outlet in the
178 Lompolojäängänoja stream (Figure 1). The sonde collected data at 30-minute intervals,
179 measuring fluorescent dissolved organic matter (FDOM), electrical conductivity, turbidity,
180 water temperature, and pH. The Finnish Environment Institute (SYKE) installed, calibrated,
181 and maintained the sensor throughout the study duration. Stream flow was measured at
182 the same location using a pressure transducer at a 120° V-notch weir, and records were
183 logged at the same temporal resolution.

184 The FDOM measurements from the sonde were used to model the concentration of DOC.
185 The instrument internally corrected for temperature effects (i.e. thermal quenching), and
186 FDOM was further corrected for turbidity using the following equation:

$$187 \quad DOC_{corrected} = \left(\frac{0.117 * fDOM}{1 - (1.1 * Turbidity) / (120 + Turbidity)} \right) \quad (1)$$

188 Here, the value 0.117 represents the slope obtained from the lab sample DOC against
189 instrument FDOM. To ensure data accuracy, regular grab samples were taken throughout
190 the study (Supplementary Figure 1). No correction was applied to the instrument for inner-
191 filter effects, as there was no observed deviation from linearity in the relationship between
192 in-stream Absorbance 254nm and stream DOC. The instrument underwent regular manual
193 cleaning every two weeks to prevent fouling, while the sensor also had a self-brushing anti-
194 fouling system. No fouling was apparent over the course of the study.

195 The calculation of DOC load during the study period was performed using the following
196 equation:

$$197 \quad C_l = C_c \cdot Q \quad (2)$$

198 Where C_l is the carbon load (mg h^{-1}), C_c is the carbon concentration (mg L^{-1}), and Q is the
199 stream flow (L h^{-1}).

200 Throughout the study, various meteorological measurements were collected. A
201 meteorological station located at the Kenttäröva forest site (Figure 1) was utilized to record
202 precipitation, snow depth, and air temperature in 10 minutes resolution. The maintenance
203 of the meteorological station was carried out by the Finnish Meteorological Institute (FMI).



204 **2.3 Data Analysis**

205

206 The 4-year dataset was transformed into hourly data by calculating hourly means. In our
207 analysis, we delineated three distinct seasonal periods: the snowmelt season, snow-free
208 season, and snow cover season.

209 The snowmelt season was defined as the period starting from the onset of snowmelt,
210 indicated by a decline in snow depth concurrent with an increase in flow, until there was no
211 remaining snow cover at the Kenttäröva site. The snow cover season referred to the period
212 when snow cover was present and persisted until the subsequent snowmelt season. The
213 snow free season referred to the period between the snowmelt and snow cover seasons. All
214 analyses were performed using R in RStudio (version 2023.03.0).

215 To conduct event-based analysis, we extracted specific events from the dataset. Events
216 were defined as periods where discharge had to exceed baseflow by 10% for a duration of
217 at least 24 hours, following definitions used in previous studies (Shogren et al., 2021;
218 Vaughan et al., 2017). Baseflow was computed using a Lyne-Hollick baseflow filter
219 implemented in the R package "grwat". In total, 92 events were identified and extracted
220 from the dataset. Among these events, 18 occurred during the snowmelt period, 63 took
221 place during the snow-free period, and 11 events were observed within the snow cover
222 period.

223 Concentration-Discharge (C-Q) analysis was performed to examine variations in transfer
224 processes at seasonal scales. We calculated the slope (β) of the logarithmic relationship
225 between DOC and streamflow (Q) for each year and each season of the study. The months
226 of December to March were not included in the seasonal analysis as flow remained at
227 baseflow during these months throughout the study. A positive slope ($\beta > 0$) suggests a
228 transport-limited relationship, indicating that the concentration of DOC is primarily
229 controlled by the transport processes. Conversely, a negative slope ($\beta < 0$) suggests a
230 source-limited relationship, indicating that the concentration of DOC is primarily influenced
231 by the sources within the catchment. A slope of zero ($\beta = 0$) indicates chemostasis,
232 indicating no significant change in DOC concentration with variations in streamflow. C-Q
233 slopes have been widely employed to assess the extent of transport or source limitation in
234 catchments (Godsey et al., 2009; Zarnetske et al., 2018).



235 Hysteresis analysis was conducted to gain insights into flow pathways and transport
236 processes at event scale. The Modified Hysteresis Index (HI) was calculated following Lloyd
237 et al., (2016b). Only single-peak events, where the flow returned to at or near baseflow,
238 were selected for analysis. The HI yielded values between -1 and 1 for each event. Positive
239 values (> 0) indicate clockwise hysteresis, where the peak concentration of DOC occurs on
240 the rising limb of the event. This pattern suggests the presence of near-stream sources or
241 rapid transport of DOC. Negative values (< 0) indicate anticlockwise hysteresis, where the
242 peak concentration of DOC occurs on the falling limb of the event. This pattern indicates the
243 influence of distal sources or slow transport of DOC (Lloyd et al., 2016b; Williams, 1989).

244 DOC load yields and event water yields were calculated for each event by totalling the sum
245 of DOC (measured in kg per km²) and water (measured in mm), and subsequent linear
246 regressions were performed to assess the variability between DOC and event water yields
247 across seasons and years (Vaughan et al., 2017). Differences in the linear regression
248 relationships signify variations in transport and source dynamics among seasons and years.
249 Furthermore, the Yield Ratio, defined as the ratio of event DOC load yield to event water
250 yield, was computed to identify potential variations between months, indicating differences
251 in transport processes (Vaughan et al., 2017).

252 To identify the best performing hydrometeorological predictors of event-based metrics, we
253 employed a machine learning method (Random Forest regression) using the R package
254 “*randomForest*”. This approach was chosen due to observed non-linearity in some of the
255 relationships. We considered a set of hydrometeorological predictors based on their
256 potential significance in prior studies examining stream nutrient concentrations across
257 seasonal timescales (Blaen et al., 2017). The selected predictor variables included maximum
258 discharge, 7-day antecedent rainfall, average air temperature during the event, average
259 water temperature during the event, and total rainfall during the event.

260 The Random Forest regressions were conducted using the entire dataset, as the aim was to
261 identify the most informative predictors. Models (names in brackets) were created to assess
262 the best predictors of Maximum event DOC (MaxDOC), the percentage of change of DOC
263 during events (DOC Change), event C-Q slope (Slope), event hysteresis index (HI), and event
264 Yield Ratio (Yield Ratio). We present the output of the models for the best predictors, as
265 determined by node purity. Higher node purity values indicate better prediction



266 performance. Additionally, we report the variance explained and the mean of squared
267 residuals for each model. These metrics provide insights into the predictive power and
268 goodness of fit of the selected predictors. Only models with variance explained > 10% are
269 featured. Resultantly, no HI models are featured, as they did not meet this threshold.

270 **3.0 Results**

271

272 **3.1 Time Series**

273 Flow exhibited a pronounced seasonal pattern (Fig. 2a). Each year, the highest flow occurred
274 during the snowmelt season. In the snow-free season, flow was primarily driven by episodic
275 precipitation events. During the early snow cover season, flow was responsive to some
276 precipitation events, but remained at baseflow for most of the snow cover season (Table 1).

277 DOC concentrations (Fig. 2b; Table 1) generally exhibited a consistent rise throughout the
278 snowmelt season, and remained elevated throughout the snow-free period, albeit with
279 frequent event-driven peaks. During the snow cover period, DOC levels initially declined and
280 then stabilized. DOC load, on the other hand, mirrored the dynamics of flow, and the
281 highest loads occurred during the snowmelt season, with smaller event-driven peaks during
282 the snow-free season.

283 Air temperature (Fig. 2c; Table 1) during the snowmelt season exhibited a positive trend,
284 with some variation around 0 °C meaning regular fluctuation between melting and freezing
285 in the snowmelt season. In the snow-free season, temperatures increased until August and
286 then declined. At the onset of the snow cover season, temperatures dropped below zero.
287 Snow cover typically began in mid-October and reached its peak in March or early April.

288 Water temperature (Fig. 2d; Table 1) remained relatively stable during most of the
289 snowmelt season and gradually increased towards the end of the period. Throughout the
290 snow-free season, water temperature closely tracked air temperature. During the snow
291 cover season, water temperature hovered around 0 °C. Turbidity, on the other hand, peaked
292 during the snowmelt season due to initial flushes, but also reached high levels during large
293 summer events in the snow-free season.

294 When considering the total annual cumulative DOC load averaged across the study (Fig. 2e;
295 Table 1), the ~6 week snowmelt period contributed around 33.4% of the total annual DOC



296 load. In contrast, the snow-free season contributed approximately 59% of the total annual
297 DOC load, while the snow cover season contributed around 7.6%.

298 **Table 1** – Hydrometeorological variables in the snow cover, snow melt, and snow free
299 seasons. Values are presented as Mean \pm Standard Deviation.

Measurement	Snow Cover	Snow Melt	Snow Free
Flow ($\text{L s}^{-1} \text{ km}^2$)	4.89 ± 4.06	34.38 ± 35.77	12.05 ± 10.90
DOC Concentration (mg L^{-1})	4.03 ± 0.99	6.39 ± 1.12	6.84 ± 1.47
DOC Load (kg h^{-1})	0.41 ± 0.50	4.62 ± 5.26	1.71 ± 1.98
Air Temperature ($^{\circ}\text{C}$)	-6.74 ± 6.03	3.62 ± 5.37	9.51 ± 6.08
Water Temperature ($^{\circ}\text{C}$)	0.18 ± 0.14	1.76 ± 3.14	9.31 ± 4.31
Turbidity (NTU)	0.91 ± 0.62	1.37 ± 0.88	0.77 ± 0.52

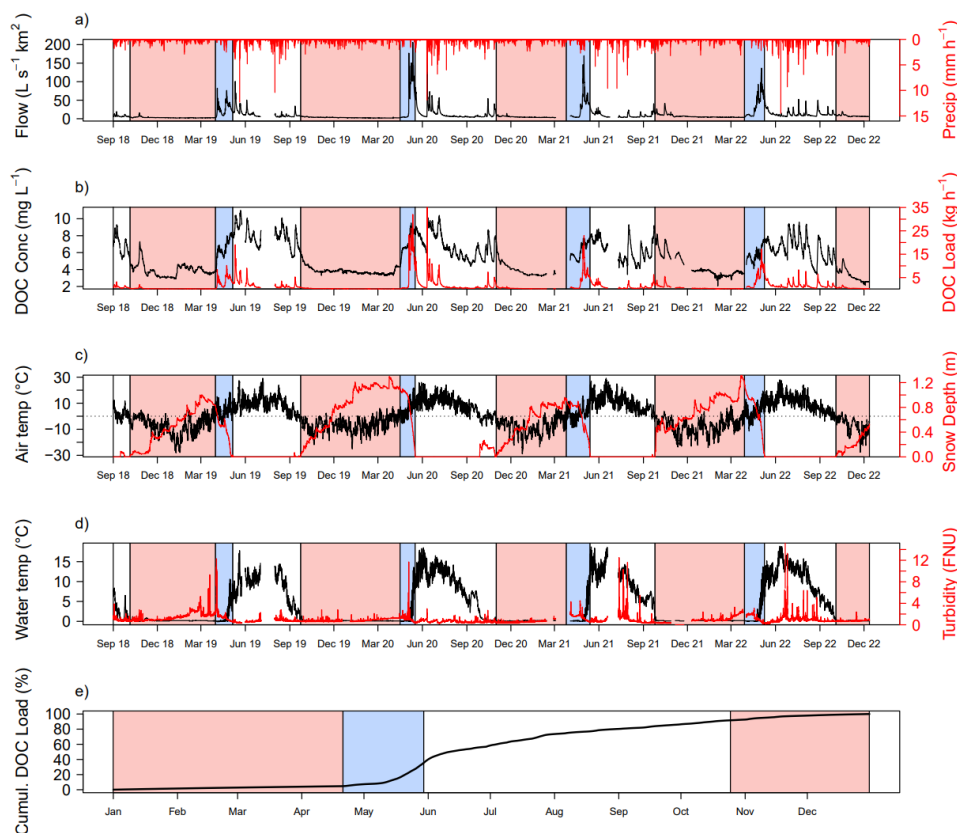
300

301

302

303

304



305

306

307 **Figure 2** – Time series depicting: a) Flow (black) and Precipitation (red), b) DOC
308 concentration (black) and DOC load (red), c) Air temperature (black) and snow depth (red),
309 d) Water temperature (black) and Turbidity (red), and e) Average cumulative DOC load for
310 the study period. The background shading indicates the different seasons: white background
311 represents the snow-free season, red background represents the snow cover season, and
312 blue background represents the snowmelt season. In graph e, the shading represents the
313 average date of the snow-free, permanent snow cover, and snowmelt seasons.

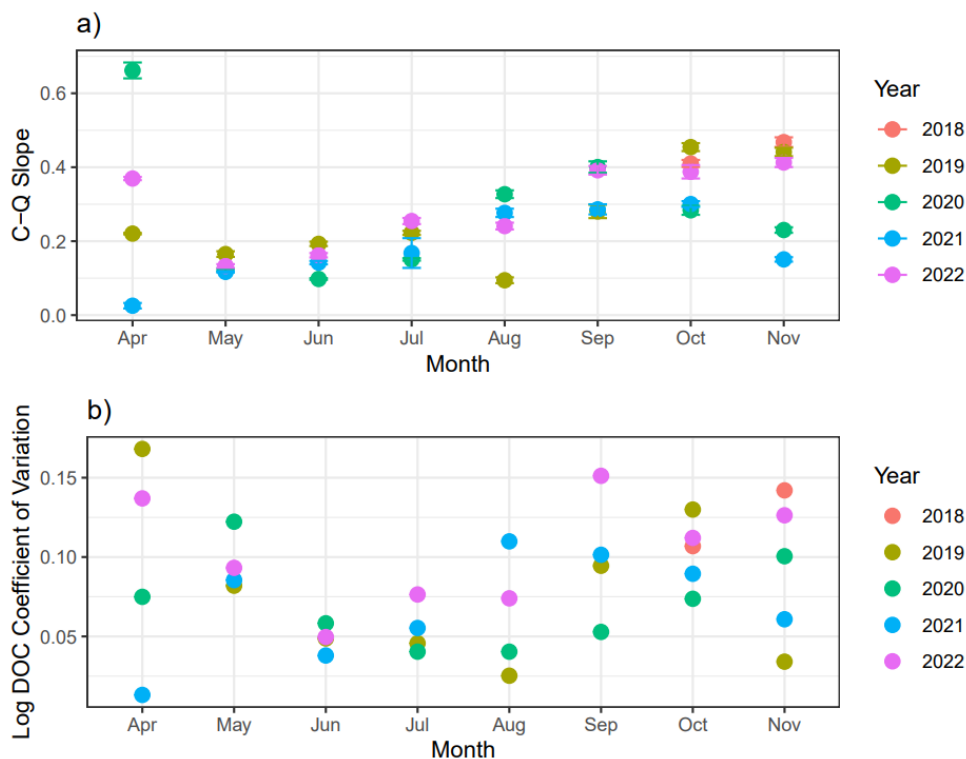
314 **3.2 Concentration-discharge (C-Q) relationships**

315 The analysis of the C-Q relationship revealed consistent positive slopes across all months
316 and years, indicating transport limitation (Fig. 3a). A pronounced seasonal trend in slope
317 was observed throughout the study period. From May to November, the slope exhibited a
318 consistent increase. In April, substantial variation in slopes was observed, primarily driven
319 by minimal flow changes in most years. Occasional outliers were noted in August 2019, and
320 November 2020 and 2021; but these were attributable to minimal range in flow in those



321 months. Notably, the variation between years was relatively small and generally smaller
322 than the month-to-month differences. The coefficient of variance data shows strong
323 seasonal and between years differences in variation of the DOC data (Fig. 3b). The largest
324 variation of DOC between years occurred during April and May, while in the summer
325 months of June to August, variation was continuously the lowest, before subsequently
326 increasing again in the Autumn months.

327 In contrast, when considering events only, the C-Q slope showed less pronounced seasonal
328 variation (Fig. 4a). No significant differences were found between months ($F = 0.77$, $P >$
329 0.05) or seasons ($F = 1.54$, $P > 0.05$), although the slope during snow cover exhibited slightly
330 higher values compared to other months. Notably, non-linear relationships emerged
331 between the C-Q slope and 7-day antecedent precipitation for flow events (Fig. 4b). During
332 the snow-free season, the slope was significantly negatively correlated with antecedent
333 precipitation up to approximately 20 mm ($R^2 = 0.26$, $P < 0.001$), beyond which the slope
334 relationship plateaued around 0 despite increasing antecedent precipitation. A similar
335 significant relationship was observed during the snow cover season ($R^2 = 0.57$, $P < 0.01$).
336 However, a no significant relationship was observed during the snowmelt season ($R^2 = 0.00$,
337 $P > 0.05$). Interestingly, the C-Q slope consistently exhibited higher values during the snow
338 cover season compared to the snow-free season.

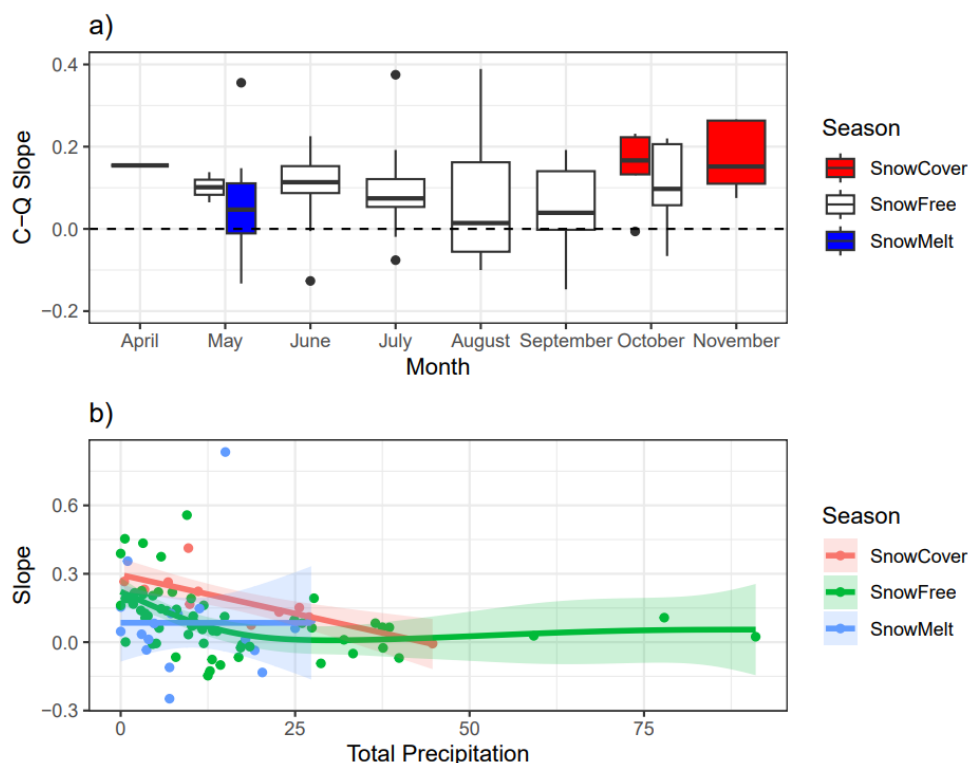


339

340

341 **Figure 3 – a)** All flow C-Q Slope Analysis. Each individual dot represents the slope of the C-Q
342 relationship for the given month. B) All Log DOC coefficient of variation. Each individual dot
343 represents the coefficient of variation for Log DOC for the given month. The year of the
344 sample is shown by the colour of the dot.

345



346

347 **Figure 4** – C-Q slope analysis for individual events. A) Boxplot of C-Q slope for events by
348 month, b) Relationship of slope of C-Q relationship with 7-day antecedent precipitation.
349 Shading shows the standard error. Dot colours show season of event, and the line shows the
350 fitted General Additive Model.

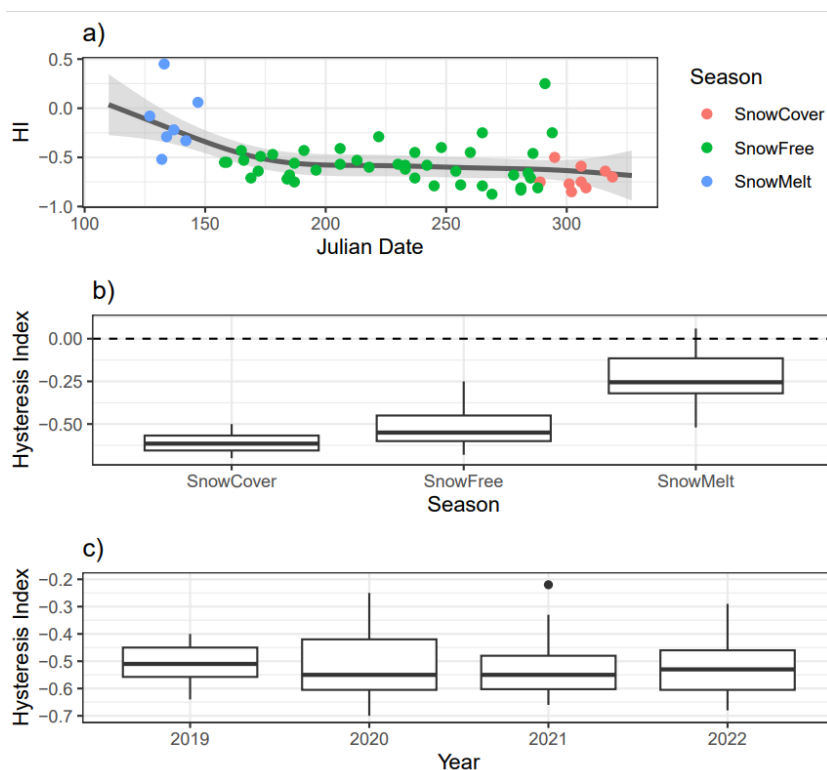
351 **Hysteresis patterns**

352 In the Hysteresis analysis, the HI exhibited significant ($R^2 = 0.28$, $P < 0.001$) and distinct
353 seasonal patterns (Fig. 5a). During the snowmelt season, HI values were generally highest,
354 ranging from weakly positive to weakly negative. However, as the season progressed and
355 transitioned into the snow-free season, HI values showed a rapid decline and remained
356 relatively consistent around -0.5. Throughout the snow cover season, HI exhibited a
357 relatively stable pattern. Notably, a single positive outlier with an HI value of 0.26 was
358 observed during the snow-free season, which can be attributed to a rare event
359 characterized by heavy early snowfall followed by subsequent rainfall.

360 Significant differences were found between the snowmelt season and snow free season ($T =$
361 5.15, $P < 0.001$), and the snowmelt season and snow cover season ($T = 5.46$, $P < 0.01$; Fig.



362 5b), indicating distinct hysteresis patterns during different periods. However, no significant
363 difference was observed between the snow cover season and the snow-free season ($T =$
364 1.76 , $P > 0.05$), suggesting similar hysteresis behaviour during these periods. Furthermore,
365 there were no significant differences in HI between different years of the study ($F = 0.51$, $P >$
366 0.05 ; Fig. 5c), indicating consistent hysteresis patterns across the study duration.
367



368

369 **Figure 5** – a) Time series of Hysteresis Index against Julian Date with the fitted general
370 additive model. Dot colours show seasons. Shading shows the standard error of the
371 predictions from the general additive model B) Boxplot showing Hysteresis Index variation
372 by season. C) Boxplot showing Hysteresis Index variation by year.

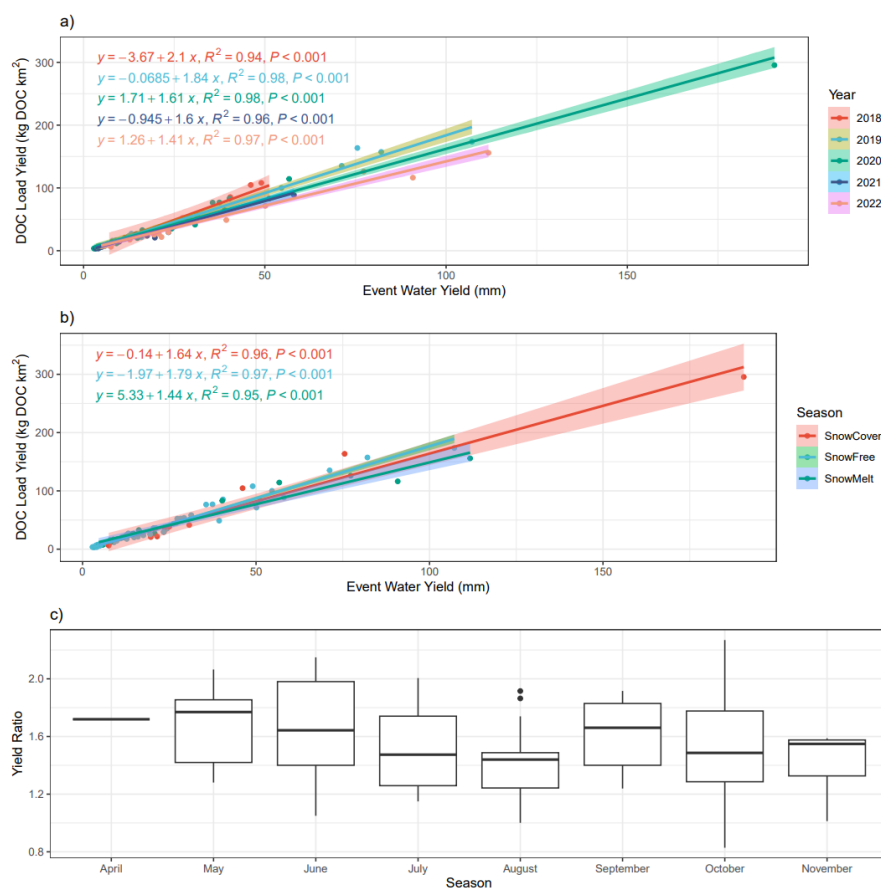
373 **3.3 DOC load and event water yields relationships**

374 The analysis of event yield revealed significant inter-annual variations in the relationship
375 between DOC load yield and Event Water Yield (Fig. 6a; $F = 7.95$, $P < 0.0001$). Specifically,
376 the regressions for 2018 and 2019 was significantly steeper than 2020 (2018 – 2020: $T =$
377 3.04 , $P < 0.05$ and 2019 – 2020: $T = 3.24$, $P < 0.05$) and 2022 (2018 – 2022: $T = 4.10$, $P < 0.01$;



378 2019 – 2022: $T = 5.19$, $P < 0.0001$), indicating differences in the transport and source
379 dynamics between these years. However, no significant differences were observed between
380 the seasons during the study ($F = 0.27$, $P > 0.05$; Fig. 6b).

381 Across all years and seasons, the relationship between DOC load yield and Event Water Yield
382 remained strongly linear (all $P < 0.001$; $R^2 = 0.91 - 0.98$). This suggests a consistent and
383 predictable relationship between the amount of dissolved organic carbon and event water
384 yield. Furthermore, the analysis of the yield ratio across months showed no apparent
385 seasonal trends (Fig. 6c), with no significant differences observed between months ($F = 1.07$;
386 $P > 0.05$).



387

388 **Figure 6** – Event yield analysis figures showing a) Linear regression of DOC load yield vs
389 Event Water Yield separated by year, b) Linear regression of DOC load yield vs Event Water
390 Yield separated by season, c) Boxplot of yield ratio for different months in study.



391 **3.4 Predictors of Seasonal Variation**

392 During the snowmelt season (Table 2a), the hydrometeorological predictors did not account
 393 for a significant amount of variation. Maximum discharge emerged as the most important
 394 predictor for both the Maximum DOC and C-Q slope models, but the predictive value of
 395 these models was relatively low (19.81% and 10.52% of variance explained, respectively).

396 In contrast, during the snow-free season (Table 2b), the predictors explained a relatively
 397 high amount of variance (55.2%) in the Maximum DOC model, with maximum discharge
 398 identified as the most important predictor (node purity = 50.19). However, for the models of
 399 DOC percentage change and yield ratio, 7-day antecedent precipitation was found to be the
 400 most important predictor, although the predictive value of these models was weak (17.68%
 401 and 11.67% of variance explained, respectively).

402 For the snow cover season (Table 2c), maximum discharge remained an important predictor
 403 for the Maximum DOC model. However, for the C-Q slope model, average water
 404 temperature and event rainfall emerged as the strongest predictors. Both the Maximum
 405 DOC and C-Q slope models showed moderate explanatory capability during the snow cover
 406 season, explaining 34.82% and 32.55% of the variance, respectively.

407 **Table 2** – Random Forest regression prediction results for target variables for a) Snow Melt
 408 Events, b) Snow Free Events, and c) Snow Cover Events. The predictor abbreviations are as
 409 follows: MaxDis = Maximum Discharge, AvgWTemp = Average Water Temperature,
 410 AvgATemp = Average Air Temperature, AntPre = 7-day antecedent precipitation, and
 411 EventPre = Total Event Precipitation. The target variables were Maximum DOC value in
 412 events (MaxDOC), the percentage DOC changed from its starting value (DOC Change), the C-
 413 Q slope of events (Slope), the Hysteresis Index (HI), and the Yield Ratio (Yield Ratio). The
 414 value in the predictors column represents the node purity. Additionally, the table presents
 415 the variance explained (%var) and the mean of squared residuals for each model (Res
 416 Mean). NS = Not significant.

a) Snow Melt							
Target	Predictors					Model	
	MaxDis	AvgW Temp	AvgA Temp	AntPre	EventPre	%Var	Res Mean
MaxDOC	3.18	2.80	2.70	2.15	1.06	19.81	0.61
DOC Change						NS	
Slope	0.227	0.14	0.15	0.07	0.04	10.52	0.04
Yield Ratio						NS	



b) Snow Free							
	Predictors					Model	
Target	MaxDis	AvgW Temp	AvgA Temp	AntPre	EventPre	%Var	Res Mean
MaxDOC	50.19	17.45	15.12	21.51	30.21	55.2	1.04
DOC Change	6712.51	5572.31	5767.61	9270.8	6113.33	17.68	523.9
Slope						NS	
Yield Ratio	1.06	0.95	0.92	1.17	0.96	11.67	0.08
c) Snow Cover							
	Predictors					Model	
Target	MaxDis	AvgW Temp	AvgA Temp	AntPre	EventPre	%Var	Res Mean
MaxDOC	1069.83	1035.79	885.8	585.89	531.53	34.82	285.6
DOC Change						NS	
Slope	0.01	0.02	0.01	0.01	0.02	32.55	0.01
Yield Ratio						NS	

417

418 **4.0 Discussion**

419 **4.1 Seasonal Variation in DOC Transport Processes**

420 Distinct seasonal variations were evident in the DOC transport processes, shedding light on
 421 their changing characteristics during different periods. Notably, the snowmelt season
 422 exhibited the lowest C-Q slope (Fig. 3a), albeit still positive, indicating a relatively lower
 423 degree of transport limitation compared to other seasons (Gómez-Gener et al., 2021). This
 424 can be attributed to the limited availability of sources during the snowmelt season
 425 (Ruckhaus et al., 2023; Shogren et al., 2021). During the snowmelt, approximately 60% of
 426 the stream water is comprised of event water, i.e., the melting snowpack (Noor et al in
 427 review). The onset of snowmelt is characterized by more rapid melting in the peatland
 428 compared to the hillslopes, while surface pathways dominate and facilitate rapid DOC
 429 transport compared to later in the year (Laudon et al., 2004). This observation is further
 430 supported by the high (positive) HI values during the snowmelt season, indicating the
 431 connectivity of new near-stream sources and the rapid flushing of DOC from the catchment
 432 during this period (Croghan et al., 2023).



433 In contrast, the relationship between snowmelt DOC load yield and event water yield (Fig.
434 6b) did not exhibit significant variation compared to other seasons. This suggests that
435 although the transport processes differed, the overall amount of DOC relative to the unit of
436 water remained relatively consistent. Thus, despite variations in sources and transport
437 mechanisms, a sustained supply of DOC was observed without deviating from linearity,
438 implying a readily available reservoir of DOC in the catchment during the snowmelt season.
439 This was possibly because of an accumulation of DOC on the top soil surface during winter
440 (Billett et al., 2006; Dyson et al., 2011). In Pallas, soil frost is relatively minimal in the
441 peatlands and soil temperature remains above zero during early winter which allows for the
442 production of DOC (Marttila et al., 2021). Furthermore, in a previous study in Pallas, top soil
443 water (up to 1 m) has been noted to be replaced two times annually (Muhic et al., 2023) -
444 firstly during the snow melt and secondly during the late summer. This also primes
445 conditions for DOC transport from the soil column during these periods, supporting our
446 observations from the stream.

447 During the snow-free season, the C-Q slopes became consistently more transport-limited as
448 the season progressed (Fig. 3a), likely due to increased source availability as the catchment
449 gradually wetted up, activating pathways and connectivity (Birkel et al., 2017; Gómez-Gener
450 et al., 2021). Additionally, enhanced microbial activity and increased vegetation breakdown
451 throughout the growing season could provide more abundant sources of DOC (Campbell et
452 al., 2022). This interpretation is partially supported by the HI, which consistently revealed
453 strong anti-clockwise hysteresis, indicative of likely distal sources and slow DOC transport
454 (Ducharme et al., 2021). However, the HI did not show significant seasonal variation across
455 the snow-free season. Notably, a steeper linear relationship between DOC yield and event
456 yield was observed during the snow-free season compared to the snowmelt season (Fig. 6b),
457 suggesting a greater supply of DOC per unit of water during events (Vaughan et al., 2017).
458 Furthermore, while maximum discharge consistently influenced DOC dynamics in all
459 seasons, antecedent precipitation emerged as an important predictor during the snowmelt
460 season, highlighting the role of prior rainfall in supporting transport dynamics (Blaen et al.,
461 2017; Tiefenbacher et al., 2021). For the C-Q slope (Fig. 3c), higher antecedent rainfall led to
462 reduced transport limitation, suggesting the exhaustion of certain sources to some extent.
463 Interestingly, the relationship was non-linear, and with high antecedent rainfall, no further



464 change in the relationship was observed, possibly indicating that high antecedent rainfall
465 enables the transport of new sources of DOC, preventing the system from becoming source
466 limited, even under extremely high antecedent precipitation or large events.

467 Surprisingly, the snow cover season (late October, November) exhibited the highest values
468 for the C-Q slope, indicating that increasing source limitation did not occur despite the
469 presence of snow cover (Fig. 3A), possibly resultant from decay of organic matter
470 dominating after the end of the growing season. Interestingly, the C-Q slope was also
471 consistently higher with antecedent rainfall during the snow cover season, compared to the
472 snow free season. This suggests that antecedent rainfall had a lesser impact on reducing
473 source supply during this period. The antecedent rainfall may also come as snow, and the
474 snowmelt vs rainfall contribution to discharge in the early snow season are difficult to
475 identify. One possible explanation is that the snow cover season begins in the hills and
476 forests, where the snow depth is recorded (Kenttäröva station Fig. 1), while the snow cover
477 on the peatland occurs later (Croghan et al., 2023; Marttila et al., 2021). Consequently,
478 during the snow cover season, the hillslopes, which likely contribute less carbon per unit of
479 water, are cut off, while the carbon-enriched peatlands make an increased contribution to
480 streamflow during events compared to other seasons (Gómez-Gener et al., 2021; Rosset et
481 al., 2019). However, neither the HI nor yield analysis showed significant variation during the
482 snow cover season. The use of spatially distributed hydrological models in future studies
483 would be valuable in identifying source contributors and further investigating if the
484 differences in source contributions during the snow cover season drive the observed
485 variations in C-Q relationships (Ala-aho et al., 2018; Birkel et al., 2017).

486 **4.2 Inter-Annual Variation in Transport Processes**

487 Despite significant year-to-year variations in hydrometeorological conditions, including
488 snow cover onset and snowmelt conditions, we found limited inter-annual variation in the
489 C-Q slope and HI (Fig. 3-5). While there were some differences in C-Q slopes between years,
490 the month-to-month variation outweighed the year-to-year variation, suggesting a
491 remarkable consistency in the degree of seasonality in transport limitation throughout the
492 study. This consistency implies activation of consistent sources and flow pathways from year
493 to year (Vaughan et al., 2017; Zarnetske et al., 2018). Similarly, the HI values showed no
494 discernible differences on an annual basis, indicating flow path stability in this system (Lloyd



495 et al., 2016b). Source activation and transport processes have a strong seasonal pattern;
496 however, the differences between years may not have been pronounced enough to drive
497 substantial changes, underscoring the need for longer-term data series for a comprehensive
498 understanding.

499 In contrast, the yield analysis revealed variations between years. Specifically, we observed
500 steeper regressions for 2018 and 2019 compared to 2020 and 2022, indicating a higher
501 transport of DOC per unit of water during these years. Thus, though source activation
502 processes do not appear to be changing year on year, the DOC yield does, which highlights
503 the need to understand how changes in water source contribution drive changes in both
504 processes and yield. Previous long-term studies have suggested that warmer years lead to
505 increased mobilization of DOC, possibly due to reduced snowpack duration which creates
506 more potential for soil C to be mobilised and a greater potential breakdown of the humic
507 layer (Bowering et al., 2023, 2020). Although 2019 was not an exceptionally warmer year,
508 we did observe a quicker onset of snowmelt peaks (Croghan et al., 2023). Consequently,
509 years with rapid snowmelt onset may result in a greater mobilization of DOC per unit of
510 water. In the longer term, the warming climate will also impact vegetation and peatland
511 formation patterns (Sallinen et al., 2023), which eventually impact also flow paths,
512 connectivity and DOC transport. Thus, highlighting the need to maintain critical
513 environmental monitoring infrastructure in high latitudes.

514 **5.0 Conclusions**

515 Our study provides valuable insights into the seasonal and inter-annual variations in DOC
516 transport processes in the Arctic, stressing the need for comprehensive monitoring across
517 all seasons. By examining various transport metrics, we observed distinct patterns that
518 enhance our understanding of carbon dynamics in Arctic ecosystems. The observed seasonal
519 variations in C-Q slopes indicate a progressive increase in transport limitation as the year
520 progresses from snowmelt to snow-free season to snow-covered season due to increased
521 source supply. The decline in hysteresis index after the snowmelt season highlights the rapid
522 flushing of DOC from the catchment during this period. Importantly, the relationship
523 between DOC yield and event water yield remained consistent across seasons, suggesting a
524 stable supply of DOC per unit of water. However, high-resolution DOC monitoring is needed
525 for improving DOC storage and transport process understanding. Interestingly, despite



526 significant year-to-year variations in hydrometeorological conditions, the intra-annual
527 variation in transport processes was relatively low. This suggests a remarkable consistency
528 in the activation and deactivation of sources and flow pathways over the study period.
529 However, longer-term records are necessary to fully comprehend the impacts of climate
530 change on DOC transport processes as headwater are anticipated to warm and water
531 sources and paths shift.

532 Our findings emphasize the vulnerability of DOC transport processes to change with snow
533 and snowmelt season in response to climate change. Our study highlights the importance of
534 long-term monitoring to assess the long-term impacts on DOC transport. To further enhance
535 our understanding, future research should focus on establishing causal relationships
536 between transport metrics and indicators of sources and transport processes, integrating
537 high-resolution stable water isotope monitoring and spatially distributed hydrological
538 modelling with *in-situ* DOC monitoring. This work contributes to advancing our knowledge
539 of DOC transport processes in Arctic ecosystems, providing valuable information for
540 informed decision-making and effective management of these fragile environments in the
541 face of climate change.

542 **Data Availability**

543 Data supporting this study are available from the corresponding author upon request.

544 **Author Contribution**

545 Conceptualization: DC, HM, PAA, KK, DMH. Formal Analysis: DC, Funding Acquisition: HM,
546 JW, BK, Investigation: DC, Resources: HM, BK, JW, JV, Visualization: DC, Writing – original
547 draft preparation: DC, Writing – review & editing: DC, PAA, JW, KRM, KK, DMH, JV, BK, HM.

548 **Competing Interests**

549 The authors declare that they have no conflict of interest.

550 **Acknowledgements**

551 The study was supported by the Maa-ja Vesitekniikan Tuki ry, the K. H. Renlund Foundation,
552 the Academy of Finland (projects: 316349, 316014, 308511, 318930, 312559, and 337552),
553 the Strategic Research Council, JMW's UArctic Research Chairship, and the University of
554 Oulu Kvantum Institute. The study is part of the activities of the National Freshwater
555 Competence Centre (FWCC).

556



557 **References**

- 558 Ala-aho, P., Soulsby, C., Pokrovsky, O. S., Kirpotin, S. N., Karlsson, J., Serikova, S., Vorobyev, S. N.,
559 Manasyrov, R. M., Loiko, S., and Tetzlaff, D.: Using stable isotopes to assess surface water source
560 dynamics and hydrological connectivity in a high-latitude wetland and permafrost influenced
561 landscape, *Journal of Hydrology*, 556, 279–293, <https://doi.org/10.1016/J.JHYDROL.2017.11.024>,
562 2018.
- 563 Anderson, L. E., DeMont, I., Dunnington, D. D., Bjorndahl, P., Redden, D. J., Brophy, M. J., and
564 Gagnon, G. A.: A review of long-term change in surface water natural organic matter concentration
565 in the northern hemisphere and the implications for drinking water treatment, *Science of The Total
566 Environment*, 858, 159699, <https://doi.org/10.1016/j.scitotenv.2022.159699>, 2023.
- 567 Argerich, A., Haggerty, R., Johnson, S. L., Wondzell, S. M., Dosch, N., Corson-Rikert, H., Ashkenas, L.
568 R., Pennington, R., and Thomas, C. K.: Comprehensive multiyear carbon budget of a temperate
569 headwater stream, *Journal of Geophysical Research: Biogeosciences*, 121, 1306–1315,
570 <https://doi.org/10.1002/2015JG003050>, 2016.
- 571 Beel, C. R., Heslop, J. K., Orwin, J. F., Pope, M. A., Schevers, A. J., Hung, J. K. Y., Lafrenière, M. J., and
572 Lamoureux, S. F.: Emerging dominance of summer rainfall driving High Arctic terrestrial-aquatic
573 connectivity, *Nature Communications*, 12, 1–9, <https://doi.org/10.1038/s41467-021-21759-3>, 2021.
- 574 Billett, M. F., Deacon, C. M., Palmer, S. M., Dawson, J. J. C., and Hope, D.: Connecting organic carbon
575 in stream water and soils in a peatland catchment, *Journal of Geophysical Research: Biogeosciences*,
576 111, <https://doi.org/10.1029/2005JG000065>, 2006.
- 577 Bintanja, R. and Andry, O.: Towards a rain-dominated Arctic, *Nature Climate Change*, 7, 263–267,
578 <https://doi.org/10.1038/nclimate3240>, 2017.
- 579 Birkel, C., Broder, T., and Biester, H.: Nonlinear and threshold-dominated runoff generation controls
580 DOC export in a small peat catchment, *Journal of Geophysical Research: Biogeosciences*, 122, 498–
581 513, <https://doi.org/10.1002/2016JG003621>, 2017.
- 582 Blaen, P. J., Khamis, K., Lloyd, C. E. M., Bradley, C., Hannah, D., and Krause, S.: Real-time monitoring
583 of nutrients and dissolved organic matter in rivers: Capturing event dynamics, technological
584 opportunities and future directions, *Science of The Total Environment*, 569–570, 647–660,
585 <https://doi.org/10.1016/J.SCITOTENV.2016.06.116>, 2016.
- 586 Blaen, P. J., Khamis, K., Lloyd, C., Comer-Warner, S., Ciocca, F., Thomas, R. M., MacKenzie, A. R., and
587 Krause, S.: High-frequency monitoring of catchment nutrient exports reveals highly variable storm
588 event responses and dynamic source zone activation, *Journal of Geophysical Research:
589 Biogeosciences*, 122, 2265–2281, <https://doi.org/10.1002/2017JG003904>, 2017.
- 590 Bokhorst, S., Pedersen, S. H., Brucker, L., Anisimov, O., Bjerke, J. W., Brown, R. D., Ehrich, D., Essery,
591 R. L. H., Heilig, A., Ingvander, S., Johansson, C., Johansson, M., Jónsdóttir, I. S., Inga, N., Luojus, K.,
592 Macelloni, G., Mariash, H., McLennan, D., Rosqvist, G. N., Sato, A., Savela, H., Schneebeil, M.,
593 Sokolov, A., Sokratov, S. A., Terzago, S., Vikhamar-Schuler, D., Williamson, S., Qiu, Y., and Callaghan,
594 T. V.: Changing Arctic snow cover: A review of recent developments and assessment of future needs
595 for observations, modelling, and impacts, *Ambio*, 45, 516–537, [https://doi.org/10.1007/s13280-016-
0770-0](https://doi.org/10.1007/s13280-016-
596 0770-0), 2016.



- 597 Bowering, K. L., Edwards, K. A., Prestegard, K., Zhu, X., and Ziegler, S. E.: Dissolved organic carbon
598 mobilized from organic horizons of mature and harvested black spruce plots in a mesic boreal
599 region, *Biogeosciences*, 17, 581–595, <https://doi.org/10.5194/bg-17-581-2020>, 2020.
- 600 Bowering, K. L., Edwards, K. A., Wiersma, Y. F., Billings, S. A., Warren, J., Skinner, A., and Ziegler, S. E.:
601 Dissolved Organic Carbon Mobilization Across a Climate Transect of Mesic Boreal Forests Is
602 Explained by Air Temperature and Snowpack Duration, *Ecosystems*, 26, 55–71,
603 <https://doi.org/10.1007/s10021-022-00741-0>, 2023.
- 604 Bring, A., Fedorova, I., Dibike, Y., Hinzman, L., Mård, J., Mernild, S. H., Prowse, T., Semenova, O.,
605 Stuefer, S. L., and Woo, M.-K.: Arctic terrestrial hydrology: A synthesis of processes, regional effects,
606 and research challenges, *Journal of Geophysical Research: Biogeosciences*, 121, 621–649,
607 <https://doi.org/10.1002/2015JG003131>, 2016.
- 608 Bruhwiler, L., Parmentier, F. J. W., Crill, P., Leonard, M., and Palmer, P. I.: The Arctic Carbon Cycle
609 and Its Response to Changing Climate, *Current Climate Change Reports*, 7, 14–34,
610 <https://doi.org/10.1007/s40641-020-00169-5>, 2021.
- 611 Campbell, T. P., Ulrich, D. E. M., Toyoda, J., Thompson, J., Munsy, B., Albright, M. B. N., Bailey, V. L.,
612 Tfaily, M. M., and Dunbar, J.: Microbial Communities Influence Soil Dissolved Organic Carbon
613 Concentration by Altering Metabolite Composition, *Frontiers in Microbiology*, 12, 2022.
- 614 Campeau, A. and del Giorgio, P. A.: Patterns in CH₄ and CO₂ concentrations across boreal rivers:
615 Major drivers and implications for fluvial greenhouse emissions under climate change scenarios,
616 *Global Change Biology*, 20, 1075–1088, <https://doi.org/10.1111/gcb.12479>, 2014.
- 617 Croghan, D., Ala-Aho, P., Lohila, A., Welker, J., Vuorenmaa, J., Kløve, B., Mustonen, K.-R., Aurela, M.,
618 and Marttila, H.: Coupling of Water-Carbon Interactions During Snowmelt in an Arctic Finland
619 Catchment, *Water Resources Research*, 59, e2022WR032892,
620 <https://doi.org/10.1029/2022WR032892>, 2023.
- 621 Csank, A. Z., Czimczik, C. I., Xu, X., and Welker, J. M.: Seasonal Patterns of Riverine Carbon Sources
622 and Export in NW Greenland, *Journal of Geophysical Research: Biogeosciences*, 124, 840–856,
623 <https://doi.org/10.1029/2018JG004895>, 2019.
- 624 Day, J. J. and Hodges, K. I.: Growing Land-Sea Temperature Contrast and the Intensification of Arctic
625 Cyclones, *Geophysical Research Letters*, 45, 3673–3681, <https://doi.org/10.1029/2018GL077587>,
626 2018.
- 627 Dick, J. J., Tetzlaff, D., Birkel, C., and Soulsby, C.: Modelling landscape controls on dissolved organic
628 carbon sources and fluxes to streams, *Biogeochemistry*, 122, 361–374,
629 <https://doi.org/10.1007/s10533-014-0046-3>, 2015.
- 630 Ducharme, A. A., Casson, N. J., Higgins, S. N., and Friesen-Hughes, K.: Hydrological and catchment
631 controls on event-scale dissolved organic carbon dynamics in boreal headwater streams,
632 *Hydrological Processes*, 35, e14279, <https://doi.org/10.1002/HYP.14279>, 2021.
- 633 Dyson, K. E., Billett, M. F., Dinsmore, K. J., Harvey, F., Thomson, A. M., Piirainen, S., and Kortelainen,
634 P.: Release of aquatic carbon from two peatland catchments in E. Finland during the spring
635 snowmelt period, *Biogeochemistry*, 103, 125–142, <https://doi.org/10.1007/s10533-010-9452-3>,
636 2011.



- 637 Finlay, J., Neff, J., Zimov, S., Davydova, A., and Davydov, S.: Snowmelt dominance of dissolved
638 organic carbon in high-latitude watersheds: Implications for characterization and flux of river DOC,
639 *Geophysical Research Letters*, 33, <https://doi.org/10.1029/2006GL025754>, 2006.
- 640 Fork, M. L., Sponseller, R. A., and Laudon, H.: Changing Source-Transport Dynamics Drive Differential
641 Browning Trends in a Boreal Stream Network, *Water Resources Research*, 56, e2019WR026336,
642 <https://doi.org/10.1029/2019WR026336>, 2020.
- 643 Godsey, S. E., Kirchner, J. W., and Clow, D. W.: Concentration-discharge relationships reflect
644 chemostatic characteristics of US catchments, *Hydrological Processes*, 23, 1844–1864,
645 <https://doi.org/10.1002/hyp.7315>, 2009.
- 646 Gómez-Gener, L., Hotchkiss, E. R., Laudon, H., and Sponseller, R. A.: Integrating Discharge-
647 Concentration Dynamics Across Carbon Forms in a Boreal Landscape, *Water Resources Research*, 57,
648 e2020WR028806, <https://doi.org/10.1029/2020WR028806>, 2021.
- 649 Koch, J. C., Sjöberg, Y., O'Donnell, J. A., Carey, M. P., Sullivan, P. F., and Terskaia, A.: Sensitivity of
650 headwater streamflow to thawing permafrost and vegetation change in a warming Arctic, *Environ.*
651 *Res. Lett.*, 17, 044074, <https://doi.org/10.1088/1748-9326/ac5f2d>, 2022.
- 652 Lambert, T., Pierson-Wickmann, A.-C., Gruau, G., Jaffrezic, A., Petitjean, P., Thibault, J. N., and
653 Jeanneau, L.: DOC sources and DOC transport pathways in a small headwater catchment as revealed
654 by carbon isotope fluctuation during storm events, *Biogeosciences*, 11, 3043–3056,
655 <https://doi.org/10.5194/bg-11-3043-2014>, 2014.
- 656 Laudon, H., Köhler, S., and Buffam, I.: Seasonal TOC export from seven boreal catchments in
657 northern Sweden, *Aquat. Sci.*, 66, 223–230, <https://doi.org/10.1007/s00027-004-0700-2>, 2004.
- 658 Laudon, H., Berggren, M., Ågren, A., Buffam, I., Bishop, K., Grabs, T., Jansson, M., and Köhler, S.:
659 Patterns and Dynamics of Dissolved Organic Carbon (DOC) in Boreal Streams: The Role of Processes,
660 Connectivity, and Scaling, *Ecosystems*, 14, 880–893, <https://doi.org/10.1007/s10021-011-9452-8>,
661 2011.
- 662 Laudon, H., Spence, C., Buttle, J., Carey, S. K., McDonnell, J. J., McNamara, J. P., Soulsby, C., and
663 Tetzlaff, D.: Save northern high-latitude catchments, *Nature Geoscience*, 10, 324–325,
664 <https://doi.org/10.1038/ngeo2947>, 2017.
- 665 Li, M., Peng, C., Zhang, K., Xu, L., Wang, J., Yang, Y., Li, P., Liu, Z., and He, N.: Headwater stream
666 ecosystem: an important source of greenhouse gases to the atmosphere, *Water Research*, 190,
667 116738, <https://doi.org/10.1016/j.watres.2020.116738>, 2021.
- 668 Liu, S., Wang, P., Huang, Q., Yu, J., Pozdniakov, S. P., and Kazak, E. S.: Seasonal and spatial variations
669 in riverine DOC exports in permafrost-dominated Arctic river basins, *Journal of Hydrology*, 612,
670 128060, <https://doi.org/10.1016/j.jhydrol.2022.128060>, 2022.
- 671 Lloyd, C. E. M., Freer, J. E., Johnes, P. J., and Collins, A. L.: Technical Note: Testing an improved index
672 for analysing storm discharge-concentration hysteresis, *Hydrol. Earth Syst. Sci.*, 20, 625–632,
673 <https://doi.org/10.5194/hess-20-625-2016>, 2016a.
- 674 Lloyd, C. E. M., Freer, J. E., Johnes, P. J., and Collins, A. L.: Using hysteresis analysis of high-resolution
675 water quality monitoring data, including uncertainty, to infer controls on nutrient and sediment
676 transfer in catchments, *Science of The Total Environment*, 543, 388–404,
677 <https://doi.org/10.1016/j.scitotenv.2015.11.028>, 2016b.



- 678 Marttila, H., Lohila, A., Ala-Aho, P., Noor, K., Welker, J. M., Croghan, D., Mustonen, K., Meriö, L.-J.,
679 Autio, A., Muhic, F., Bailey, H., Aurela, M., Vuorenmaa, J., Penttilä, T., Hyöky, V., Klein, E., Kuzmin, A.,
680 Korpelainen, P., Kumpula, T., Rauhala, A., and Kløve, B.: Subarctic catchment water storage and
681 carbon cycling – leading the way for future studies using integrated datasets at Pallas, Finland,
682 *Hydrological Processes*, <https://doi.org/10.1002/HYP.14350>, 2021.
- 683 Marttila, H., Laudon, H., Tallaksen, L. M., Jaramillo, F., Alfredsen, K., Ronkanen, A.-K., Kronvang, B.,
684 Lotsari, E., Kämäri, M., Ala-Aho, P., Nousu, J., Silander, J., Koivusalo, H., and Kløve, B.: Nordic
685 hydrological frontier in the 21st century, *Hydrology Research*, 53, 700–715,
686 <https://doi.org/10.2166/nh.2022.120>, 2022.
- 687 Mcguire, A. D., Anderson, L. G., Christensen, T. R., Scott, D., Laodong, G., Hayes, D. J., Martin, H.,
688 Lorenson, T. D., Macdonald, R. W., and Nigal, R.: Sensitivity of the carbon cycle in the Arctic to
689 climate change, *Ecological Monographs*, 79, 523–555, <https://doi.org/10.1890/08-2025.1>, 2009.
- 690 McGuire, A. D., Lawrence, D. M., Koven, C., Clein, J. S., Burke, E., Chen, G., Jafarov, E., MacDougall, A.
691 H., Marchenko, S., Nicolsky, D., Peng, S., Rinke, A., Ciais, P., Gouttevin, I., Hayes, D. J., Ji, D., Krinner,
692 G., Moore, J. C., Romanovsky, V., Schädell, C., Schaefer, K., Schuur, E. A. G., and Zhuang, Q.:
693 Dependence of the evolution of carbon dynamics in the northern permafrost region on the
694 trajectory of climate change, *Proceedings of the National Academy of Sciences of the United States*
695 *of America*, 115, 3882–3887, <https://doi.org/10.1073/pnas.1719903115>, 2018.
- 696 Metcalfe, D. B., Hermans, T. D. G., Ahlstrand, J., Becker, M., Berggren, M., Björk, R. G., Björkman, M.
697 P., Blok, D., Chaudhary, N., Chisholm, C., Classen, A. T., Hasselquist, N. J., Jonsson, M., Kristensen, J.
698 A., Kumordzi, B. B., Lee, H., Mayor, J. R., Prevéy, J., Pantazatou, K., Rousk, J., Sponseller, R. A.,
699 Sundqvist, M. K., Tang, J., Uddling, J., Wallin, G., Zhang, W., Ahlström, A., Tenenbaum, D. E., and
700 Abdi, A. M.: Patchy field sampling biases understanding of climate change impacts across the Arctic,
701 *Nature Ecology and Evolution*, 2, 1443–1448, <https://doi.org/10.1038/s41559-018-0612-5>, 2018.
- 702 Muhic, F., Ala-Aho, P., Noor, K., Welker, J. M., Kløve, B., and Marttila, H.: Flushing or mixing? Stable
703 water isotopes reveal differences in arctic forest and peatland soil water seasonality, *Hydrological*
704 *Processes*, 37, e14811, <https://doi.org/10.1002/hyp.14811>, 2023.
- 705 Osuch, M., Wawrzyniak, T., and Majerska, M.: Changes in hydrological regime in High Arctic non-
706 glaciated catchment in 1979–2020 using a multimodel approach, *Advances in Climate Change*
707 *Research*, 13, 517–530, <https://doi.org/10.1016/j.accre.2022.05.001>, 2022.
- 708 Pearson, R. G., Phillips, S. J., Loranty, M. M., Beck, P. S. A., Damoulas, T., Knight, S. J., and Goetz, S. J.:
709 Shifts in Arctic vegetation and associated feedbacks under climate change, *Nature Climate Change*,
710 3, 673–677, <https://doi.org/10.1038/nclimate1858>, 2013.
- 711 Pedron, S. A., Jespersen, R. G., Xu, X., Khazindar, Y., Welker, J. M., and Czimczik, C. I.: More Snow
712 Accelerates Legacy Carbon Emissions From Arctic Permafrost, *AGU Advances*, 4, e2023AV000942,
713 <https://doi.org/10.1029/2023AV000942>, 2023.
- 714 Prokushkin, A. S., Pokrovsky, O. S., Shirokova, L. S., Korets, M. A., Viers, J., Prokushkin, S. G., Amon, R.
715 M. W., Guggenberger, G., and McDowell, W. H.: Sources and the flux pattern of dissolved carbon in
716 rivers of the Yenisey basin draining the Central Siberian Plateau, *Environmental Research Letters*, 6,
717 45212–45226, <https://doi.org/10.1088/1748-9326/6/4/045212>, 2011.
- 718 Pulliainen, J., Luoju, K., Derksen, C., Mudryk, L., Lemmetyinen, J., Salminen, M., Ikonen, J., Takala,
719 M., Cohen, J., Smolander, T., and Norberg, J.: Patterns and trends of Northern Hemisphere snow



- 720 mass from 1980 to 2018, *Nature* 2020 581:7808, 581, 294–298, [https://doi.org/10.1038/s41586-](https://doi.org/10.1038/s41586-020-2258-0)
721 020-2258-0, 2020.
- 722 Rantanen, M., Karpechko, A. Y., Lipponen, A., Nordling, K., Hyvärinen, O., Ruosteenoja, K., Vihma, T.,
723 and Laaksonen, A.: The Arctic has warmed nearly four times faster than the globe since 1979,
724 *Commun Earth Environ*, 3, 1–10, <https://doi.org/10.1038/s43247-022-00498-3>, 2022.
- 725 Räsänen, A., Manninen, T., Korkiakoski, M., Lohila, A., and Virtanen, T.: Predicting catchment-scale
726 methane fluxes with multi-source remote sensing, *Landscape Ecology*, 36, 1177–1195,
727 <https://doi.org/10.1007/S10980-021-01194-X/FIGURES/4>, 2021.
- 728 Rosset, T., Gandois, L., Le Roux, G., Teisserenc, R., Duranwez Jimenez, P., Camboulive, T., and Binet,
729 S.: Peatland Contribution to Stream Organic Carbon Exports From a Montane Watershed, *Journal of*
730 *Geophysical Research: Biogeosciences*, 124, 3448–3464, <https://doi.org/10.1029/2019JG005142>,
731 2019.
- 732 Ruckhaus, M., Seybold, E. C., Underwood, K. L., Stewart, B., Kincaid, D. W., Shanley, J. B., Li, L., and
733 Perdrial, J. N.: Disentangling the responses of dissolved organic carbon and nitrogen concentrations
734 to overlapping drivers in a northeastern United States forested watershed, *Frontiers in Water*, 5,
735 2023.
- 736 Sallinen, A., Akanegbu, J., Marttila, H., and Tahvanainen, T.: Recent and future hydrological trends of
737 aapa mires across the boreal climate gradient, *Journal of Hydrology*, 617, 129022,
738 <https://doi.org/10.1016/j.jhydrol.2022.129022>, 2023.
- 739 Shatilla, N. J. and Carey, S. K.: Assessing inter-annual and seasonal patterns of DOC and DOM quality
740 across a complex alpine watershed underlain by discontinuous permafrost in Yukon, Canada,
741 *Hydrology and Earth System Sciences*, 23, 3571–3591, <https://doi.org/10.5194/hess-23-3571-2019>,
742 2019.
- 743 Shogren, A. J., Zarnetske, J. P., Abbott, B. W., Iannucci, F., and Bowden, W. B.: We cannot shrug off
744 the shoulder seasons: Addressing knowledge and data gaps in an Arctic headwater, *Environmental*
745 *Research Letters*, 15, 104027, <https://doi.org/10.1088/1748-9326/ab9d3c>, 2020.
- 746 Shogren, A. J., Zarnetske, J. P., Abbott, B. W., Iannucci, F., Medvedeff, A., Cairns, S., Duda, M. J., and
747 Bowden, W. B.: Arctic concentration–discharge relationships for dissolved organic carbon and nitrate
748 vary with landscape and season, *Limnology and Oceanography*, 66, S197–S215,
749 <https://doi.org/10.1002/lno.11682>, 2021.
- 750 Speetjens, N. J., Tanski, G., Martin, V., Wagner, J., Richter, A., Hugelius, G., Boucher, C., Lodi, R.,
751 Knoblauch, C., Koch, B. P., Wunsch, U., Lantuit, H., and Vonk, J. E.: Dissolved organic matter
752 characterization in soils and streams in a small coastal low-Arctic catchment, *Biogeosciences*, 19,
753 3073–3097, <https://doi.org/10.5194/bg-19-3073-2022>, 2022.
- 754 Tan, A., Adam, J. C., and Lettenmaier, D. P.: Change in spring snowmelt timing in Eurasian Arctic
755 rivers, *Journal of Geophysical Research: Atmospheres*, 116, D03101,
756 <https://doi.org/10.1029/2010JD014337>, 2011.
- 757 Tank, S. E., Striegl, R. G., McClelland, J. W., and Kokelj, S. V.: Multi-decadal increases in dissolved
758 organic carbon and alkalinity flux from the Mackenzie drainage basin to the Arctic Ocean,
759 *Environmental Research Letters*, 11, 054015, <https://doi.org/10.1088/1748-9326/11/5/054015>,
760 2016.



- 761 Tiefenbacher, A., Weigelhofer, G., Klik, A., Mabit, L., Santner, J., Wenzel, W., and Strauss, P.:
762 Antecedent soil moisture and rain intensity control pathways and quality of organic carbon exports
763 from arable land, *CATENA*, 202, 105297, <https://doi.org/10.1016/j.catena.2021.105297>, 2021.
- 764 Vaughan, M. C. H., Bowden, W. B., Shanley, J. B., Vermilyea, A., Sleeper, R., Gold, A. J., Pradhanang,
765 S. M., Inamdar, S. P., Levia, D. F., Andres, A. S., Birgand, F., and Schroth, A. W.: High-frequency
766 dissolved organic carbon and nitrate measurements reveal differences in storm hysteresis and
767 loading in relation to land cover and seasonality, *Water Resources Research*, 53, 5345–5363,
768 <https://doi.org/10.1002/2017WR020491>, 2017.
- 769 Vihma, T., Screen, J., Tjernström, M., Newton, B., Zhang, X., Popova, V., Deser, C., Holland, M., and
770 Prowse, T.: The atmospheric role in the Arctic water cycle: A review on processes, past and future
771 changes, and their impacts, *Journal of Geophysical Research: Biogeosciences*, 121, 586–620,
772 <https://doi.org/10.1002/2015JG003132>, 2016.
- 773 Ward, A. S., Wondzell, S. M., Schmadel, N. M., and Herzog, S. P.: Climate Change Causes River
774 Network Contraction and Disconnection in the H.J. Andrews Experimental Forest, Oregon, USA,
775 *Frontiers in Water*, 2, 2020.
- 776 Williams, G. P.: Sediment concentration versus water discharge during single hydrologic events in
777 rivers, *Journal of Hydrology*, 111, 89–106, [https://doi.org/10.1016/0022-1694\(89\)90254-0](https://doi.org/10.1016/0022-1694(89)90254-0), 1989.
- 778 de Wit, H. A., Valinia, S., Weyhenmeyer, G. A., Futter, M. N., Kortelainen, P., Austnes, K., Hessen, D.
779 O., Råike, A., Laudon, H., and Vuorenmaa, J.: Current Browning of Surface Waters Will Be Further
780 Promoted by Wetter Climate, *Environ. Sci. Technol. Lett.*, 3, 430–435,
781 <https://doi.org/10.1021/acs.estlett.6b00396>, 2016.
- 782 Zarnetske, J. P., Bouda, M., Abbott, B. W., Saiers, J., and Raymond, P. A.: Generality of Hydrologic
783 Transport Limitation of Watershed Organic Carbon Flux Across Ecoregions of the United States,
784 *Geophysical Research Letters*, 45, 11,702–11,711, <https://doi.org/10.1029/2018GL080005>, 2018.
- 785